Ray tracing of optically modified fiber tips. 2: laser scalpels

Rudolf M. Verdaasdonk and Cornelius Borst

The spatial irradiance distribution of tapered fibers and tapered rods used as scalpels in laser surgery has been calculated by ray tracing. The results were compared to measurements in air and in water. The beam profiles of laser scalpels were conically shaped at discrete angles related to the number of reflections within the scalpel. Light started to leak radially out of the scalpel before it reached the tip slightly suppressing the increase in fluence rate toward the tip. For effective tissue cutting, the scalpel tip may be shortened to optimize the irradiance increase in combination with radial energy leakage to obtain controlled hemostatic coagulation. *Key words:* Laser surgery, laser scalpels, fibers optics, ray tracing.

I. Introduction

Various laser sources are being used in surgery.[1] Although highly absorbed wavelengths like CO_2 laser light (10.6 μm) cut biological tissue most efficiently, wavelengths that are less absorbed by tissue can still be used for cutting when the beam is focused to a small spot of high irradiance.[2] High fluence rates of laser light may be obtained by focusing the beam by a lens or by guiding the beam through the tapered end of a fiber[3] or a tapered rod[4–6] (Fig. 1). As the cross-sectional area of the rod decreases, the fluence rate increases until the beam begins to refract out of the taper with a large divergence angle. In contact with tissue, the point of the tapered end can be used to cut.[4] Because of the large divergence angle of the exit beam, the irradiance decreases rapidly distal from the tip minimizing injury to adjacent tissue.[5]

The optical behavior of the laser scalpels depends on the geometry of the scalpel, the beam diameter and beam divergence, the refractive index of the probe, and the refractive index of the medium. By means of ray tracing,[7] the optical behavior of laser scalpels was analyzed in relation to their geometry to determine the irradiance distribution and fluence rate within and at the tip of the scalpel. For commercially available laser scalpels, computed beam profiles were compared with photographed profiles in water.

The authors are with the University Hospital Utrecht, Heart–Lung Institute, Postbus 85500, NL-3508 GA, Utrecht, The Netherlands.

Received 26 June 1990.
0003-6935/91/162172-06$05.00/0.

II. Methods

The geometry of the tapered laser scalpels was defined by the taper angle α [Fig. 1(A)]. The scalpels were assumed to be made of sapphire having a refractive index of 1.75. The taper angle was varied from 1 to 45°. Ray tracing was performed as described in the preceding paper.[7] In brief, from points equally divided along a line on the front surface of a fiber, rays were emitted equally divided over a 10° divergence angle of a fiber. The use of a weight factor describing the relative magnitude of the rays emitted at a certain angle with respect to the normal of the fiber end resulted in an irradiance distribution which was uniform in the near field and Gaussian in the far field of the fiber. At every transition which an individual ray encountered, either the total reflectance angle or the refraction angle was calculated according to Fresnels laws of reflection and refraction[8] depending on the angle of incidence and the refractive index of the environment (Fig. 2). In case of refraction, the intensity loss due to reflection at the transition was neglected because for angles of incidence up to 30°, it is below 10% in air and below 3% in water (Fig. 2).

Depending on its starting angle and its position relative to the optical axis, a ray will reflect several times up and down the scalpel before its angle with respect to the scalpel surface exceeds the angle of total reflection. Then the ray refracts (leaks) out of the scalpel [Fig. 1(A)]. The irradiance distribution and the total energy were calculated at twenty equally spaced cross sections along twice the length of the leaking part of the scalpel. The irradiance distributions were combined to an isoirradiance level map[7] within the scalpel point. This map also displays the irradiance distribution at the tip when the point has been shortened to a particu-

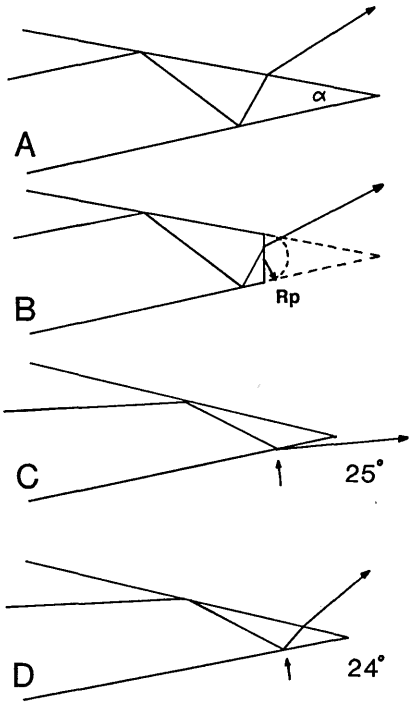

Fig. 1. (A) Ray reflected up and down inside a tapered rod with angle α until the angle of incidence relative to the surface exceeds the critical angle and the ray is refracted out of the scalpel. (B) Point of the tapered rod may be shortened to the level where the first ray refracts. It may end in either a flat or a spherical point with radius R_p. (C), (D) Decreasing the taper angle from 25 to 24° resulted in one additional internal reflection of a ray that was originally refracted out of the scalpel. Note the shift in the location of the reflection with respect to the original point of refraction (arrows) when the angle was decreased. Note also the large change in divergence.

lar level. The scalpel may end either in a flat tip with a diameter $2R_p$ or in a hemispherical tip with a radius R_p [Fig. 1(B)]. The increase in irradiance at the tip of shortened scalpels was calculated in air and in water normalized to the irradiance at the tip of a bare fiber I_f.

Table I. Dimensions of Tapered Probe Sapphire Laser Scalpels Fitted on a 0.6-mm Fiber

probe type	length probe [mm]	angle point degrees	radius point [mm]	entrance diameter [mm]
MTRP 1.5	1.5	53	0.1	1.0
MTRP 3.0	3.0	27	0.1	1.0
MTRP 5.0	5.0	16	0.1	1.0
flat scalpel	29	3.8	0.275	2.5

A. Measurements

The scalpels (Surgical Laser Technologies, Malvern, PA) which were analyzed are listed in Table I. The beam profiles of the probes were photographed as described previously.

III. Results

The commercially available scalpels, their beam profiles in water, and their calculated profiles are shown in Fig. 3. The beam profile of the small taper angle scalpel with a flat point is shown in Fig. 4.

The calculated radius of the scalpel at the level where the first rays refracted out of the scalpel in relation to the taper angle is shown in Fig. 5(A). This radius was normalized with respect to the radius of either the fiber or the entrance of the scalpel rod. The leak radius changed in large discrete steps. In air, the rays reflected further down into the scalpel tip than in water. At the leak radius, the increase in irradiance relative to the level at the entrance plane of the scalpel was calculated. For taper angles as small as 3°, the calculated normalized increase was 85 in air and 55 in water [Fig. 5(B)]. Assuming the scalpel end to be hemispherical rather than flat [Fig. 1(B)], the maximum irradiance increase was 10–30% smaller due to internal reflection losses [Fig. 5(C)].

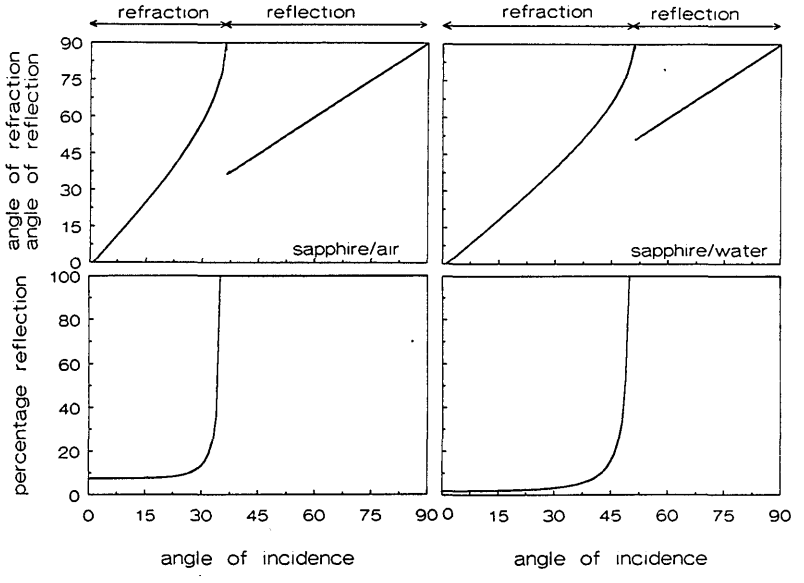

Fig. 2. Upper panel: relation between the angle of incidence and the angle of either reflection or refraction when light is incident on a transition of sapphire to air (left) and sapphire to water (right). Lower panel: the percentge of the light reflected in relation to the angle of incidence is given for sapphire/air (left) and sapphire/water (right) transitions.

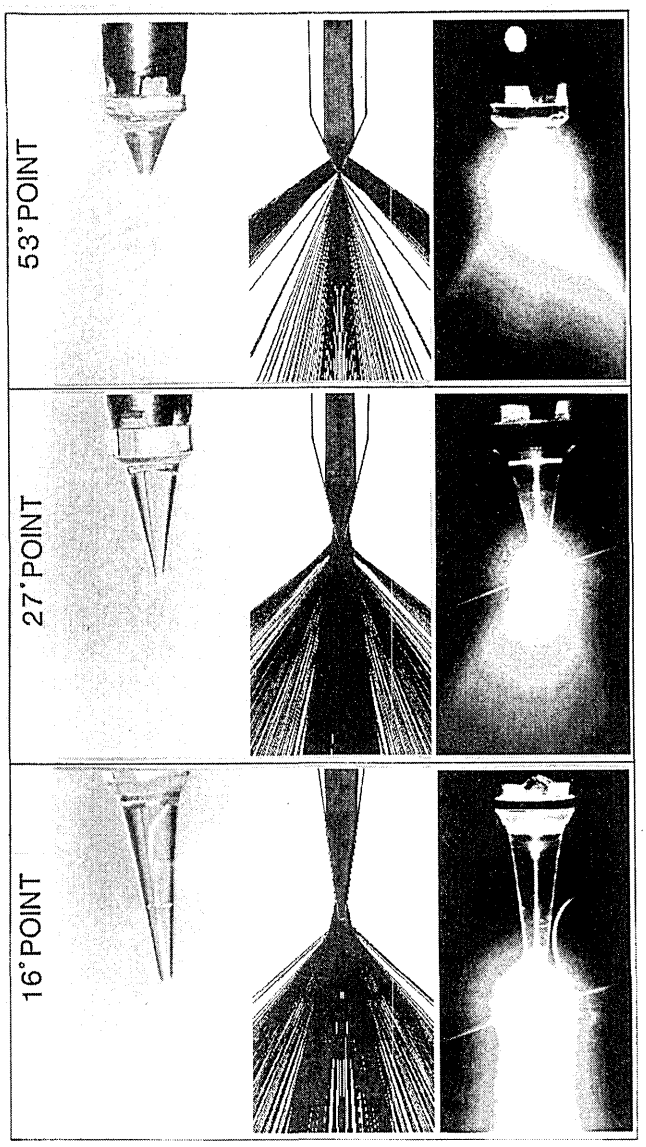

Fig. 3. Beam profiles of sapphire laser scalpels (Surgical Laser Technologies, Malvern, PA) in water. From left to right panel: scalpel, calculated beam, photographed beam. Upper panel: MTRP 1.5, taper angle 53°. Middle panel: MTRP 3.0, taper angle 27°. Lower panel: MTRP 5.0, taper angle 16°.

For taper angles of 5, 10, 15, 20, and 30°, the isoirradiance maps are presented in Fig. 6. Figure 7 displays the concurrent power reduction (A) and irradiance increase (B) toward the scalpel tip. The distance to the tip was again normalized to the leaking length of the scalpel.

IV. Discussion

A. Beam Profiles

It was difficult to visualize the total beam profile from a tapered tip due to the high irradiance at the tip outshining the diverging beam. The beam was partly scattered due to irregularities or a coating on the tip. These irregularities cannot be prevented since a very thin tapered tip will be damaged easily. The best

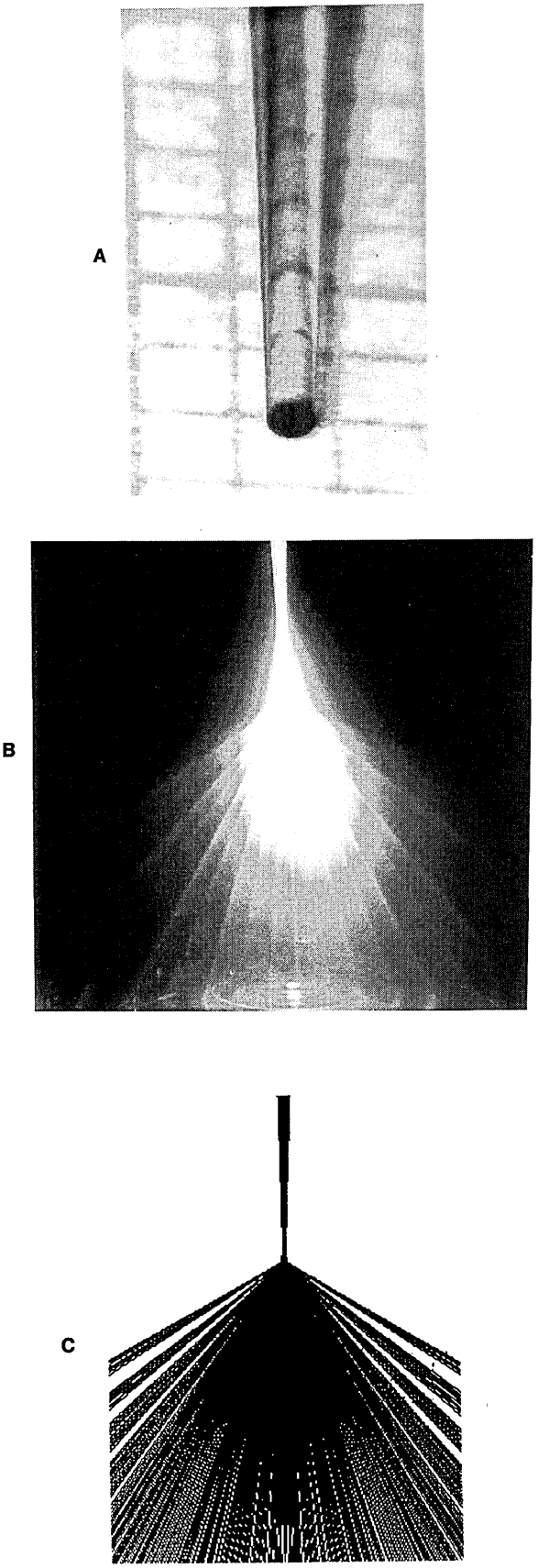

Fig. 4. (A) Flat ended scalpel with a taper angle of 3.8°. (B) Beam in water showing conically shaped beams at discrete angles. (C) Calculated beam profile in water.

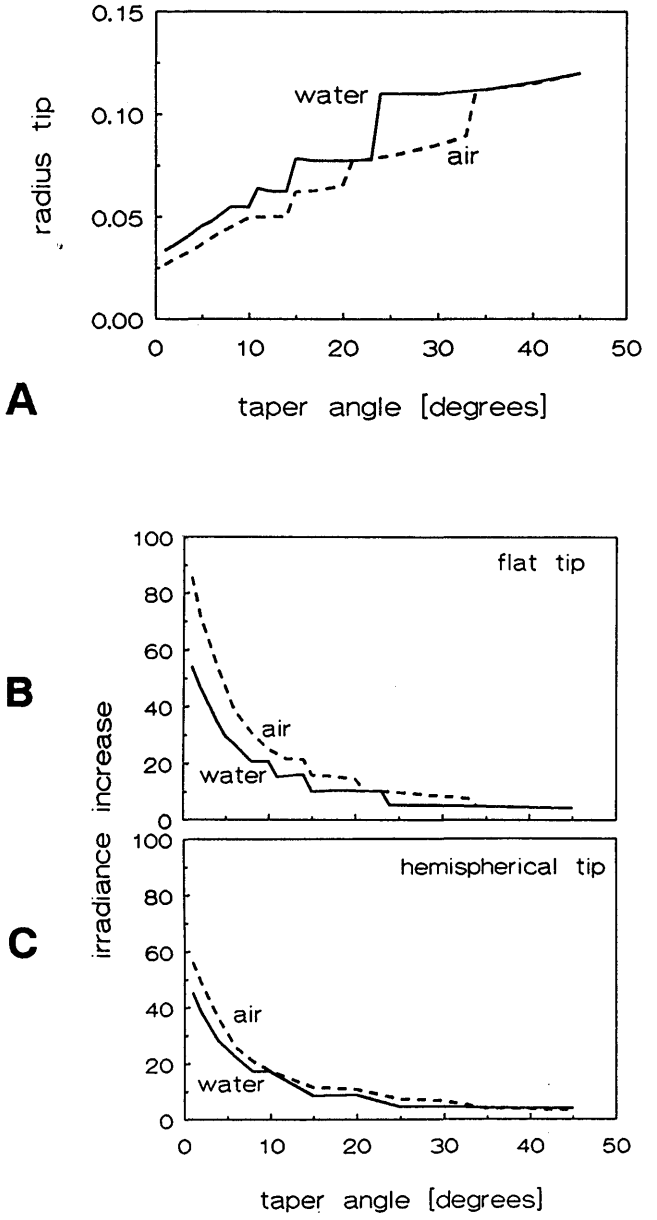

Fig. 5. (A) Radius of the tapered rod at the position where rays start to refract out of the scalpel [see Fig. 1 (A)] in relation to the taper angle in air (dotted curve) and water (solid curve). The radius was normalized with respect to the radius at the entrance of the rod. In air the rays reflect further down into the scalpel tip compared to a water environment. The steps in the curves are related to the number of reflections inside the scalpel before a ray refracts out of the scalpel. (B) Increase in irradiance relative to the bare fiber tip at the position where rays start to refract out of the scalpel for flatly tipped tapered fibers in relation to the taper angle in air and water. (C) Increase in irradiance for hemispherical tipped tapered fibers was ~10–30% smaller than in (B) due to internal reflection losses.

results were obtained in water due to index matching (Fig. 3). The beam shape was conical. This shape was most pronounced at larger taper angles. As far as can be distinguished, the calculated and photographed profiles were similar. The modified scalpel with a flat point showed several conically shaped beams at discrete angles in accordance with the profile calculated by ray tracing [Figs. 4(B) and (C)]. These angles were related to the number of reflections a ray makes inside

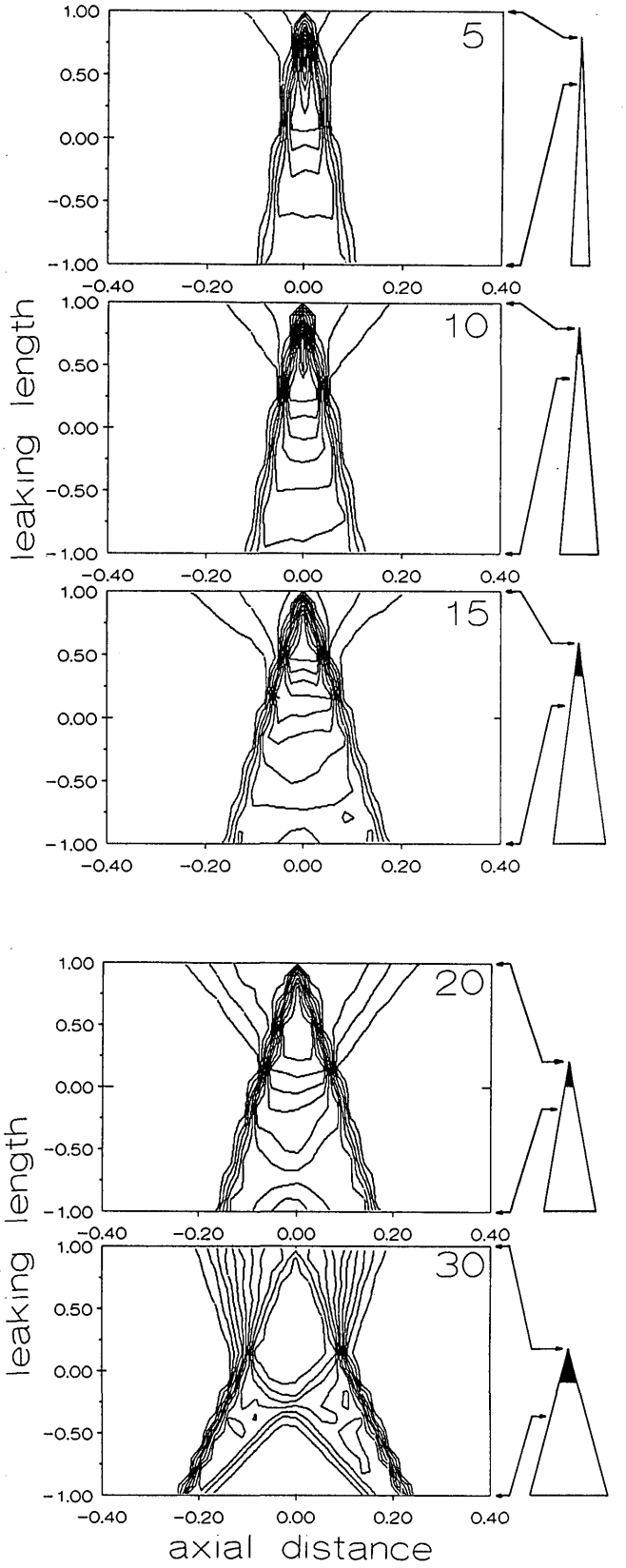

Fig. 6. Isoirradiance maps composed from twenty power distributions at equally spaced levels along the scalpel tip for 5, 10, 15, 20, and 30° taper angles. Ordinate: length scalpel normalized with respect to the leaking length (start leaking to taper end, 0–1). Abscissa: diameter scalpel in normalized to the entrance diameter of the scalpel. Next to the maps, the actual shapes of the scalpels are shown indicating the leaking length (solid) and the part presented in the isoirradiance map.

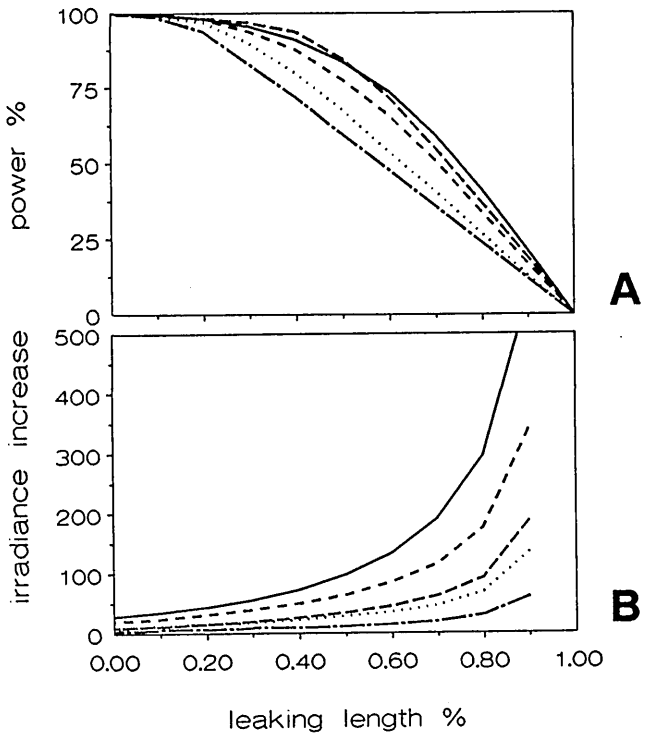

Fig. 7. (A) Reduction of the total power in percentage of the original power at the entrance of the scalpel in relation to the normalized leaking length (0–1) of the scalpel for 5, 10, 15, 20, and 30° taper angles (highest to lowest curve, respectively). (B) Corresponding increase in irradiance relative to the irradiance at the entrance of the scalpel for 5, 10, 15, 20, and 30° taper angles (highest to lowest curve, respectively).

the scalpel before it refracted out of the scalpel. The angle of each cone depended on the starting position of a ray relative to the optical axis and on its starting angle.

B. Leaking Level of Scalpel

Dependent on the taper angle, the radius of the scalpel where rays started to leak out changed in discrete steps [Fig. 5(A)]. The steps are related to the number of reflections a ray makes inside the scalpel. A small decrease in taper angle resulted in one additional internal reflection of a ray [Figs. 1(C) and (D)]. Considering the percentage of the light that is reflected near the critical angle (Fig. 2), the step will not be as abrupt as shown in Fig. 5(A). The assumption, however, that reflections below the critical angle can be neglected is fair up to an angle ~5° smaller than the critical angle where the percentage reflection will always be below 10% (Fig. 2). Once rays started to refract out of the scalpel, the total power decreased toward the tip. For smaller taper angles, more light will be reflected further toward the tip [Fig. 7(A)]. The crossing of some curves in Fig. 7(A) is due to normalization. Combined with the decrease of the cross-sectional surface area of the tip, the average irradiance increased more than a hundredfold relative to the irradiance at the entrance of the scalpel [Fig. 7(B)]. The increase in irradiance is slightly diminished by the decrease in total power inside the scalpel and by the actual dimensions of the point of the tip which cannot become infinitely small.

The isoirradiance maps (Fig. 6) show that the position and the dimensions of the area of highest irradiance depend on the taper angle. For large taper angles, the irradiance did not increase dramatically once the scalpel started leaking [Fig. 7(B)]. For small taper angles, in contrast, the highest irradiance was concentrated in the very tip. Due to limited spatial resolution of the ray tracing, the isoirradiance maps are not totally symmetrical and the peak irradiance could not be represented accurately.

The irradiance at the scalpel point may be controlled by shortening the tip of the scalpels to the level of the desired irradiance increase. If the point is cut flat, the point has sharp edges like a bare fiber. Calculation of the irradiance increase for flat ended [Fig. 5(B)] and spherically tipped scalpels [Fig. 5(C)] showed that internal reflections introduced losses in the latter. These losses were 20–30% in air and 10–20% in water. Since the scalpel is used in contact with tissue, the optical behavior in water is most appropriate to consider.[9]

The highest irradiance increase was obtained with the smallest angle of the point. A small taper angle, however, may result in a brittle and sharp point, but a taper angle of 3.8° is still feasible (Fig. 4).

C. Probe Design

The laser may be used as an alternative for the surgical knife when it is preferred for its higher precision and its hemostatic effects.[6] For some applications, for example, in eye surgery,[10] it may be the only tool available. One other advantage is the capability of combining cutting with coagulating. Using a wavelength with a high tissue penetration depth like Nd:YAG,[11,12] small blood vessels in highly perfused organs will be coagulated during cutting. In this way surgical procedures like liver resections[13] may be performed with minimal loss of blood.

For this purpose the scalpel may be shortened to a level with a high irradiance to cut effectively in combination with a sufficient leaking length for adequate hemostasis. Surgical Laser Technologies has designed scalpels with a coating to increase radial coagulation.

V. Conclusion

Beam profiles of laser scalpels are conically shaped. The discrete angles of the beams are related to the number of reflections inside the scalpel. The increase in irradiance inside the scalpels toward the tip is slightly suppressed by refraction of light out of the scalpel before the light reaches the tip and by the mechanical strength of a tip with a small taper angle. The scalpel tip may be shortened to obtain the optimum irradiance distribution with a sufficient irradiance increase for effective tissue cutting together with radial energy leaking to obtain controlled coagulation and hemostasis of the cut tissue.

The authors thank M.J.C. van Gemert and A.G.J.M. van Leeuwen for their valuable comments on the manuscript. We thank E.O. Robles de Medina for his contribution to the laser angioplasty program.

R.M.V. and the laser angioplasty program in our institute were supported by The Netherlands Heart Foundation (grants 34.001 and 87.073) and the Interuniversity Cardiology Institute of the Netherlands.

References

1. T. J. Wiemann, "Lasers and the Surgeon," Am. J. Surg. **151,** 493–500 (1986).
2. A. J. Welch, "Laser Irradiation of Tissue," in *Heat Transfer in Medicine and Biology, Vol. 2,* A. Shitzer and R. C. Eberhart, Eds **R. C. Eberhart, Eds.** (Plenum, New York, 1985), pp. 135–184.
3. C. T. Chang and D. C. Auth, "Radiation Characteristics of a Tapered Cylindrical Optical Fiber," J. Opt. Soc. Am. **68,** 1191–1196 (1978).
4. J. Hukki, I. Krogerus, M. Castren, and T. Schroder, "Effects of Different Contact Laser Scalpels on Skin and Subcutaneous Fat," Lasers Surg. Med. **8,** 276–282 (1988).
5. L. Y. Kim, Jr., A. L. Day, S. J. Normann, G. S. Abela, and J. L. Mehta, "The Argon Contact Laser Scalpel: a Study of its Effect on Atherosclerosis," Neurosurgery **21,** 861–866 (1987).
6. L. Y. Kim, Jr., T. E. Roxey, and A. L. Day, "The Argon "Contact" Laser Scalpel: Technical Considerations," Neurosurgery **21,** 858–860 (1987).
7. R. M. Verdaasdonk and C. Borst, "Ray Tracing of Optically Modified Fiber Tips. 1: Spherical Probes," Appl. Opt. **30,** 2159–2171 (1991).
8. E. Hecht and A. Zajac, *Optics* (Addison-Wesley, Reading, MA, 1979), pp. 60–98.
9. F. P. Bolin, L. E. Preuss, R. C. Taylor, and R. J. Ference, "Refractive Index of Some Mammalian Tissues Using a Fiber Optic Cladding Method," Appl. Opt. **28,** 2297–2303 (1989).
10. M. A. Mainster, *Ophthalmic Laser Surgery: Principles, Technology and Techniques* (Mosby, St. Louis, 1984), pp. 81–101.
11. H. Rosenfeld and R. Sherman, "Treatment of Cutaneous and Deep Vascular Lesions with the Nd:YAG Laser," Lasers Surg. Med. **6,** 20–23 (1986).
12. N. Daikuzono and S. N. Joffe, "Artificial Sapphire Probe for Contact Photocoagulation and Tissue Vaporization with the Nd:YAG Laser," Med. Instrum. **192,** 173–178 (1985).
13. S. N. Joffe, "Resection of the Liver with the Nd:YAG Laser," Surg. Gyn. Obstet. **163,** 437–442 (1986).